Korean J. Chem. Eng., 37(6), 1020-1028 (2020)
DOI: 10.1007/s11814-020-0547-9

pISSN: 0256-1115
eISSN: 1975-7220

Improved biodegradation of polyvinyl alcohol by hybrid nanoflowers of degrading enzymes from *Bacillus niacini*

Hongjie Bian*,, Gaoyang Wang**, Mengfei Cao*, Ziyuan Wang**, and Jiandong Cui**,†**

*Research Center for Fermentation Engineering of Hebei, College of Bioscience and Bioengineering, Hebei University of Science and Technology, 26 Yuxiang Street, Shijiazhang 050000, P. R. China
**State Key Laboratory of Food Nutrition and Safety, Laboratory of Industrial Fermentation Microbiology, Ministry of Education, Tianjin University of Science and Technology, No 29, 13th, Avenue, Tianjin Economic and Technological Development Area (TEDA), Tianjin 300457, P. R. China
(*Received 31 January 2020 • accepted 18 March 2020*)

Abstract−Polyvinyl alcohol (PVA) is a synthetic polymer that is difficult to degrade in nature. In this study, we synthesized PVA-degrading enzymes (PVAase)-$Cu_3(PO_4)_2$ hybrid nanoflowers by using crude PVAase from *Bacillus niacini* for PVA degradation. The influences of PVAase concentration, Cu^{2+} concentration, and incubation time on the nucleation and activity of the PVAase hybrid nanoflower were investigated. The maximal activity recovery of the PVAase hybrid nanoflower was approximately 85% at 0.25 mg/mL of PVAase, 0.36 mM Cu^{2+}, and 72 h incubation time. The optimum temperature and pH of PVAase did not change before and after immobilization. Compared with free PVAase, the PVAase hybrid nanoflower showed high thermal stability and storage stability. Additionally, the PVAase hybrid nanoflower displayed excellent reusability after eight cycles and promising PVA degradability, indicating its potential application in PVA degradation.

Keywords: Polyvinyl Alcohol, Biodegradation, Hybrid Nanoflower, Immobilization Enzyme, Purification

INTRODUCTION

As a synthetic polymer with desirable physical and chemical characteristics, Poly(vinyl alcohol) (PVA) is widely applied in textile industries, adhesives, and other applications [1,2]. Recently, PVA has been attracted more and more attention in the field of nanomaterials production [3,4]. However, it has become a major pollutant of theenvironment because it is difficult to degrade [5,6]. Although PVA can be degraded by high temperatures and strong oxidants, this method is energy consuming and will cause environmental pollution again. In comparison, the biodegradability of PVA by microbial enzymes would provide a promising and alternative method for PVA degradation [7,8]. Microorganisms with PVA-degrading ability have been isolated from the natural environment. For example, several strains isolated from soil exhibited the ability to degrade PVA such as *Pseudomonas* O-3 [9], *Flammulina velutipes* [10], and *Bacillus niacini* [11]. It was found that *Fomitopsis pinicola* strain (a fungal strain) could also degrade PVA [1]. Many efforts have demonstrated that the PVA-biodegradation by bacterial strains relies on PVA-degrading enzyme (PVAase) [2,12]. Mechanisms for the degradation of the main chain of PVA molecules by PVAase have been proposed [13]. Briefly, the carbon-carbon linkages of PVA (two adjacent secondary hydroxy groups) are first dehydrogenated by a dehydrogenase and then hydrolyzed by a hydrolase (Fig. 1). So far, it is difficult to realize industrial application of the PVAase. This result may be due to several reasons: (1) The production and activity of PVAase in PVA-degrading bacteria are too low; (2) free PVAase lacks long-term operational stability; and (3) it is difficult to purify the PVAase from PVA-degrading bacteria due to the complexity of PVAase (including PVA oxidase, dehydrogenase, and hydrolase) [14]. Therefore, many efforts have been made to improve the production and activity of the PVAase. For example, PVA hydrolase from *Sphingopyxis* sp. 113P3 was expressed in *Escherichia coli*, and exhibited activity the recombinant strain [15]. Jia et al. reported the expression of PVA dehydrogenase from *Sphingopyxis* sp. 113P3 in *Pichia pastoris* GS115 [16]. A three-stage fermentation strategy was

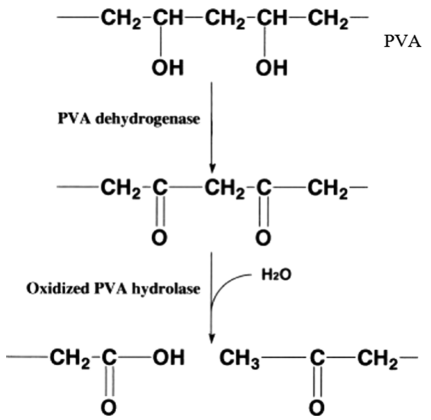


Fig. 1. Proposed mechanism of PVA degrading enzyme and its products. Figure was reproduced from Ref. [11] with permission from copyright holders.

†To whom correspondence should be addressed.
E-mail: cjd007cn@163.com
Copyright by The Korean Institute of Chemical Engineers.

developed by adding PVA to improve the productivity of PVAase [17]. Specific activity of the PVAase was significantly increased. Min et al. developed a pH control strategy to enhance PVAase production [18]. Although the production and activity of the PVAase are partly improved, PVA degradation efficiency is still low for the industrial application. Especially, the poor operational stability of free PVAase has seriously hampered its industrial application.

Generally, immobilization of enzyme is an important method to improve its stability. Furthermore, the immobilized enzymes can be recycled and reused. Therefore, immobilized enzymes are more suitable for industrial application compared with free enzymes. Immobilized technologies usually include adsorption, covalent conjugation, entrapment, and cross-linking [19]. Generally, the activity of enzymes decreases after they are immobilized [20]. Furthermore, complex purification process before immobilization also leads to loss of enzyme activity. Therefore, it is necessary to develop a simple and efficient approach for enzyme immobilization. Recently, enzyme-inorganic hybrid nanoflowers were developed for the first time by Ge et al. [21]. Subsequently, trypsin, horseradish peroxidise, lipase, papain, laccase, and α-glycosidase were immobilized by enzyme-inorganic hybrid nanoflowers [22-27]. All these hybrid nanoflowers display higher activity and stability than free enzymes. Furthermore, hybrid nanoflowers can even be prepared using the crude enzyme extract instead of the purified enzyme. Yu et al. reported a simple method for preparing soybean peroxidase-inorganic hybrid nanoflowers by using crude soybean peroxidase [28]. The resultant peroxidase hybrid nanoflowers was 4.46-fold higher activity than free crude soybean peroxidase. The recombinant β-glucosidase linker-elastin-like polypeptide-His (GLEH) from crude fermentation broth was also successfully prepared into hybrid nanoflowers. The resultant GLEH nanoflowers showed outstanding operation stability and recyclability [29]. Herein, we successfully synthesized PVAase-$Cu_3(PO_4)_2$ hybrid nanoflowers by using crude PVAase from *Bacillus niacini* for the first time. The preparation conditions of the PVAase-$Cu_3(PO_4)_2$ hybrid nanoflowers were optimized. The properties of the PVAase hybrid nanoflowers were also investigated. Finally, PVA degradation capacity and stabilities of the PVAase hybrid nanoflowers were also evaluated.

MATERIALS AND METHODS

1. Extraction of PVAase from PVA-degrading Strains

Bacillus niacini with PVAase activity was inoculated in the Luria-Bertani medium broth (containing 0.1% PVA) at 30 °C with 200 rpm for 72 h. After centrifugation, the recovered cells were disrupted by sonication in 10 mM potassium phosphate buffer (pH 7.5). After centrifugation (10,000 *g*, 15 min), 80% $(NH_4)_2SO_4$ was mixed with the supernatant for 1 h. The resultant precipitate was recovered by centrifugation, and dissolved in 10 mM phosphate buffer (pH 7.5). This crude PVAase was used to prepare hybrid nanoflowers.

2. Preparation of PVAase-$Cu_3(PO_4)_2$ Hybrid Nanoflowers

PVAase-$Cu_3(PO_4)_2$ nanoflowers were synthesized on the basis of a previous report [25]. 2 mL of $CuSO_4$ solution was added to 0.1 M phosphate buffer solution (pH 7.5) containing the crude PVAase. The mixture solution was incubated at 4 °C for 72 h. After centrifugation, the precipitates were dried by lyophilization. The influences of the crude PVAase concentration (0.05, 0.1, 0.15, 0.2, 0.25, and 0.3 mg/mL), incubation time (12, 24, 48, 72, and 96 h), and $CuSO_4$ concentration (12, 24, 36, 48, and 60 mM) on the morphology and activity of nanoflowers were investigated, respectively.

3. Protein Concentration Determination and PVAase Activity Assay

The protein amounts in solution before and after the immobilization were determined with the Bradford method [30]. PVAase activity was determined as the previous report [11]. Briefly, a number of enzyme samples were added into 0.1 M phosphate buffer (pH 8.0) containing 0.1% PVA. The reaction was performed at 30 °C for 3 h. One unit PVAase activity was defined as an absorbance decrease of 0.001 per minute at 645 nm. The PVAase activity recovery in hybrid nanoflowers was calculated as given in Eq. (1).

$$\text{Activity recovery (\%)} = \frac{\text{Total activity of hybrid nanoflowers (U)}}{\text{Total free PVAase activity used for hybrid nanoflowers production (U)}} \times 100\% \quad (1)$$

4. PVA Degradation Efficiency

PVA in the reaction solution was determined on the basis of the previous report [31]. The method is based on the green color produced by reaction of PVA with iodine in the presence of boric acid. The wave length of maximum spectrophotometric absorbance of the system is about 645 nm. 1 g/L PVA was dissolved in PVAase solution, 4% boric acid, and I_2-KI (12.7 g/L I2 and 25 g/L KI). The reaction was carried out at 30 °C for 3 h. After centrifugation, the absorbance of PVA in supernatants was determined at 645 nm. PVA degradation efficiency was calculated by using Eq. (2).

$$\text{PVA degradation efficiency (\%)} = \frac{A_0 - A_1}{A_0} \times 100\% \quad (2)$$

Here, A_0 represents OD_{645} of samples, A_1 is OD_{645} of control.

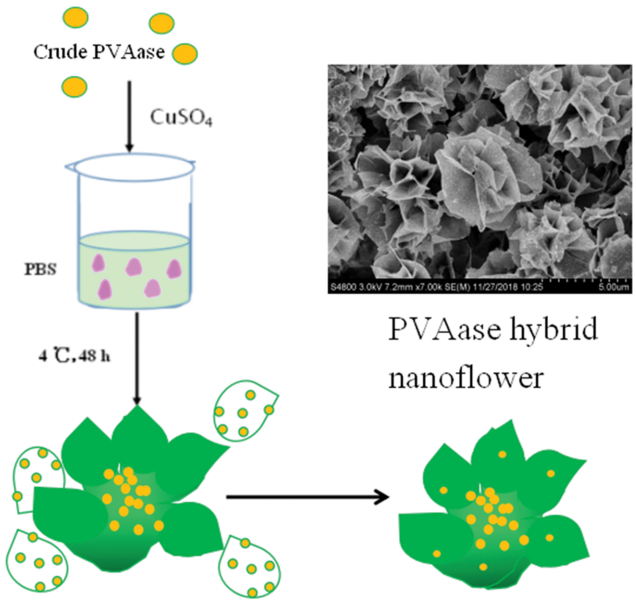


Fig. 2. Schematic of the preparation process for PVAase-$Cu_3(PO_4)_2$ hybrid nanoflowers.

5. Effects of Temperature and pH on Activity of PVAase-$Cu_3(PO_4)_2$ Hybrid Nanoflowers

The effects of temperature (30-70 °C) on activity of the nanoflowers were measured by incubating the hybrid nanoflowers in the substrate solution (1 g/L PVA) for 3 h. Effects of pH (5, 6, 7, 8, and 9) on activity of the nanoflowers were investigated by adding the hybrid nanoflowers into the substrate solution at 30 °C for 3 h. PVAase activity was determined.

6. Stability of the PVAase Hybrid Nanoflowers

Thermostability of the hybrid nanoflowers and free PVAase was measured by incubating them at 0.1 M PBS buffer (pH 7.0) for 1-5 h. The storage stability of the hybrid nanoflowers and free PVAase was determined at 25 °C. The reusability of PVAase hybrid nanoflowers was evaluated by carrying out continuous cycles using 0.1% PVA solution as the substrate. In addition, PVA degradation efficiency of PVAase hybrid nanoflowers and free PVAase was also compared using 1 g/L PVA solution as the substrate.

RESULTS AND DISCUSSION

1. Preparation and Characterization of the PVAase Hybrid Nanoflowers

Generally, the self-assembly of the hybrid nanoflowers includes three steps (Fig. 2): first, primary crystals of copper phosphate are formed. Then, PVAase proteins attach to copper phosphate crystals through coordination. Finally, anisotropic growth leads to the formation of nanoflowers [32,33]. In this study, the effects of PVAase concentration on the nucleation of the hybrid nanoflowers were investigated. As shown in Fig. 3, no nanoflowers were observed when the concentration of PVAase was 0.05 mg/mL, 0.1 mg/mL, and 0.15 mg/mL (Fig. 3(a), 3(b), and 3(c)), respectively. However, particles with flower structure were observed when the concentra-

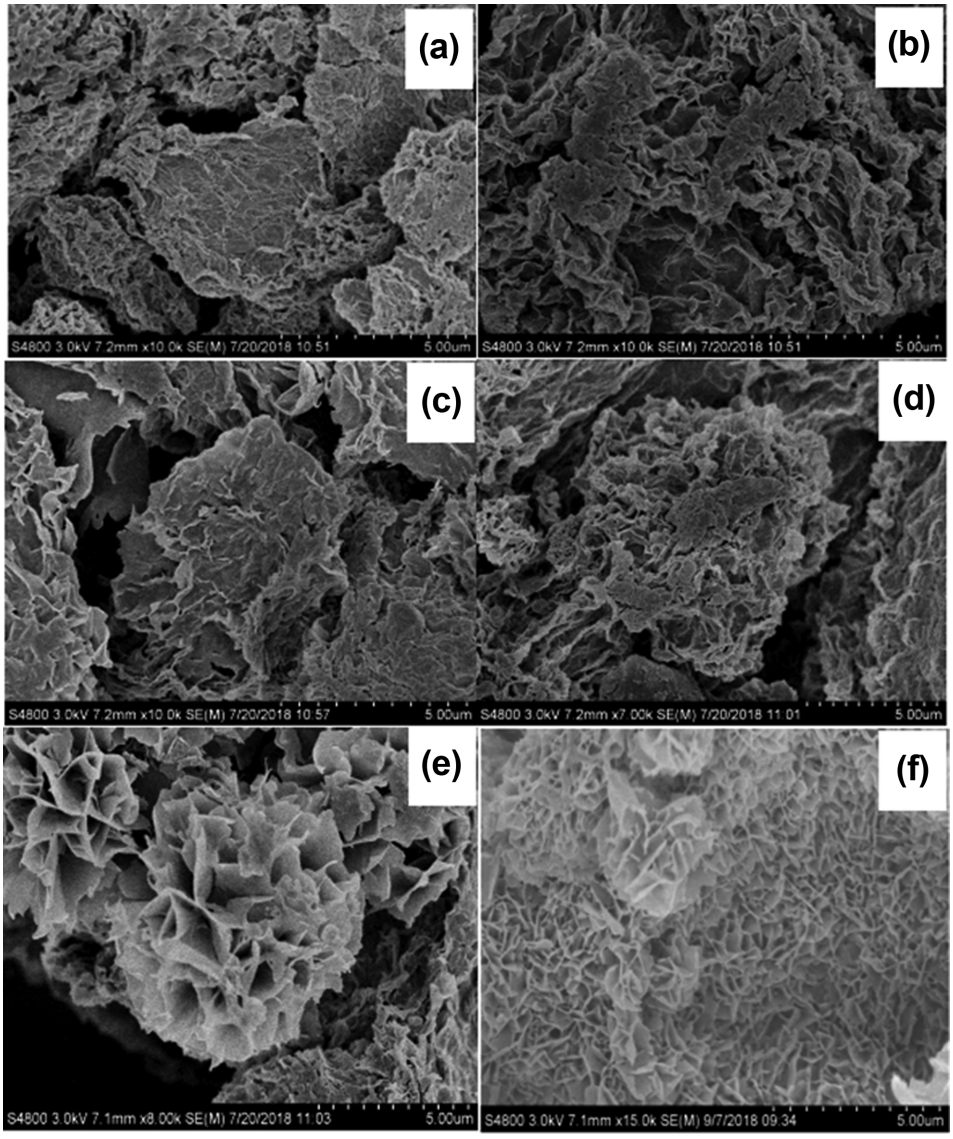


Fig. 3. SEM images of effects of PVAase concentration on morphology of PVAase hybrid nanoflowers. (a) 0.05 mg/mL, (b) 0.1 mg/mL, (c) 0.15 mg/mL, (d) 0.2 mg/mL, (e) 0.25 mg/mL, (f) 0.3 mg/mL.

tion of PVAase was 0.2 mg/mL (Fig. 2(d)). With further increase of PVAase concentration (0.25 mg/mL), uniform nanoflowers were formed (Fig. 3(e)). However, large aggregates with scattered petals were observed when PVAase concentration reached 0.3 mg/mL) (Fig. 3(f)). These results confirmed that PVAase concentration plays a crucial role in regulating the formation of hybrid nanoflowers. Similar phenomena were also found in the literature [34,35]. The effects of Cu^{2+} concentration on the morphology of the PVAase hybrid nanoflowers are shown in Fig. 4. At low concentration of copper ion (<24 mM), large crystals, but no nanoflowers were formed (Fig. 4(a), 4(b)). However, small buds emerged when Cu^{2+} concentration was increased to 36 mM (Fig. 4(c)). Complete nanoflowers were observed (Fig. 4(d)) when Cu^{2+} concentration was 48 mM. Large blooming nanoflowers appeared when Cu^{2+} concentration was 60 mM (Fig. 4(e)). Similarly, incubation time also exhibited a significant effect on morphology of the PVAase hybrid nanoflowers. Before 36 h, only primary crystals of $Cu_3(PO_4)_2$ were formed (Fig. 5(a), 5(b)). At 48 h, PVAase-Cu^{2+} combined into complexes, and formed the primary petals (Fig. 5(c)). Subsequently, anisotropic growth led to complete formation of a flower-like structure at 72 h (Fig. 5(e)). However, a further increase in incubation time (96 h) resulted in large flower-like aggregates. These results indicated that the morphology of the hybrid nanoflowers was significantly affected by PAVase concentration, Cu^{2+} concentration, and

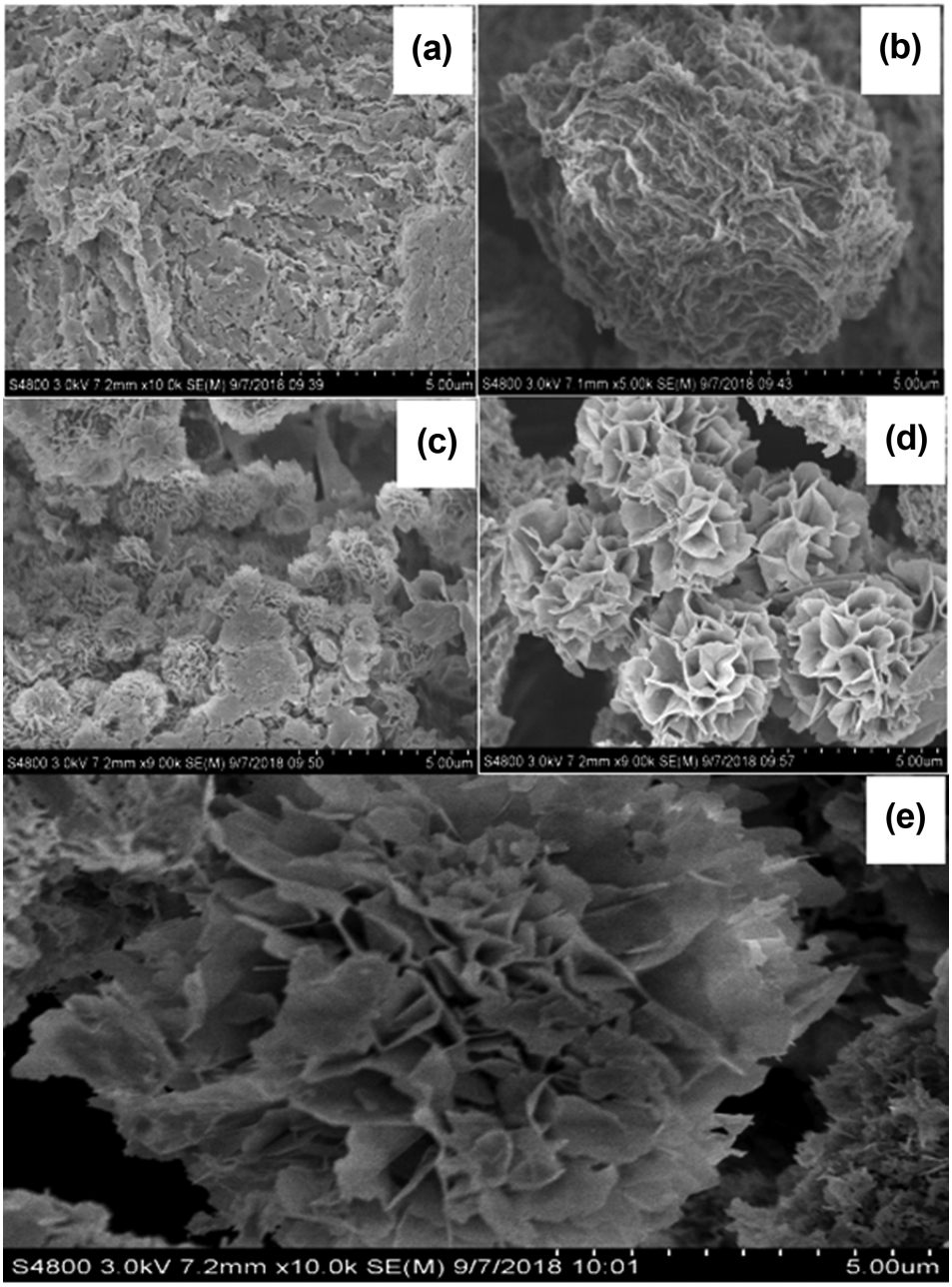


Fig. 4. SEM images of effects of $CuSO_4$ concentration on morphology of PVAase hybrid nanoflowers. (a) 12 mM, (b) 24 mM, (c) 36 mM, (d) 48 mM, (e) 60 mM.

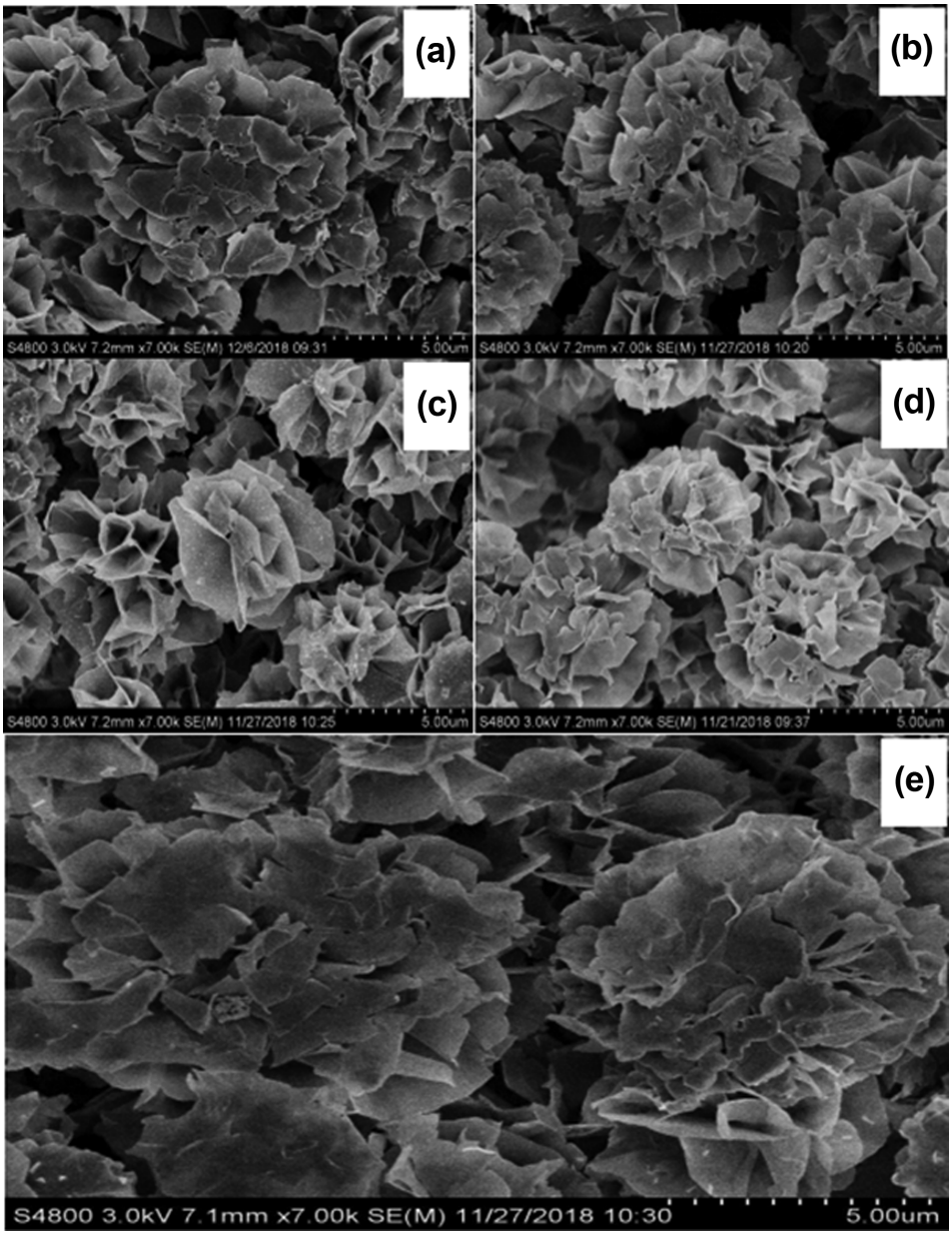


Fig. 5. SEM images of effects of incubation time on morphology of PVAase hybrid nanoflowers. (a) 24 h, (b) 36 h, (c) 48 h, (d) 72 h, (e) 96 h.

incubation time. TEM image showed that nanoflowers are formed by interlaced nanoplates in Fig. 6. The high magnification TEM images showed that the nanoplates consisted of individual inorganic nanoparticles ($Cu_3(PO_4)_2$) and organic component (PVAase). The $Cu_3(PO_4)_2$ nanoparticles were bound by PVAase (Fig. 6(c)). These results were consistent with previous reports [36,37]. Fluorescence micrograph using FITC labeled PVAase showed that PVAase was embedded in the nanoplates of hybrid nanoflowers because the labeled PVAase exhibited a typical green fluorescence (Fig. 6(d)). To further confirm the presence of PVAase molecules in the hybrid nanoflowers, the chemical structures of free PVAase and PVAase hybrid nanoflowers were also measured by FTIR. Characteristic peak at 1,640 cm^{-1} in free PVAase and the PVAase hybrid nanoflowers was attributed to amide I in proteins, indicating the presence of PVAase molecules in the hybrid nanoflowers (Fig. 7(a)). Characteristic absorption at 1,050 cm^{-1} and 933 cm^{-1} was ascribed to P-O vibrations [28], suggesting the existence of phosphate groups in the hybrid nanoflowers. XRD analysis revealed that the diffraction peaks of the PVAase hybrid nanoflowers at 7.5°, 13.0°, 31.5°, 28.7°, and 53.5° were consistent with those of the standard $Cu_3(PO_4)_2 3H_2O$ (JPSCD 00-022-0548) (Fig. 7(b)), thus further demonstrating the presence of $Cu_3(PO_4)_2$ in the PVAase hybrid nanoflowers.

2. Catalytic Activity of the PVAase Hybrid Nanoflowers

Effects of PVAase concentration, Cu^{2+} concentration, and incubation time on the activity of the PAVase hybrid nanoflowers were studied. The results are shown in Fig. 8(a). PVAase concentration had significant effects on activity of the PVAase hybrid nanoflower.

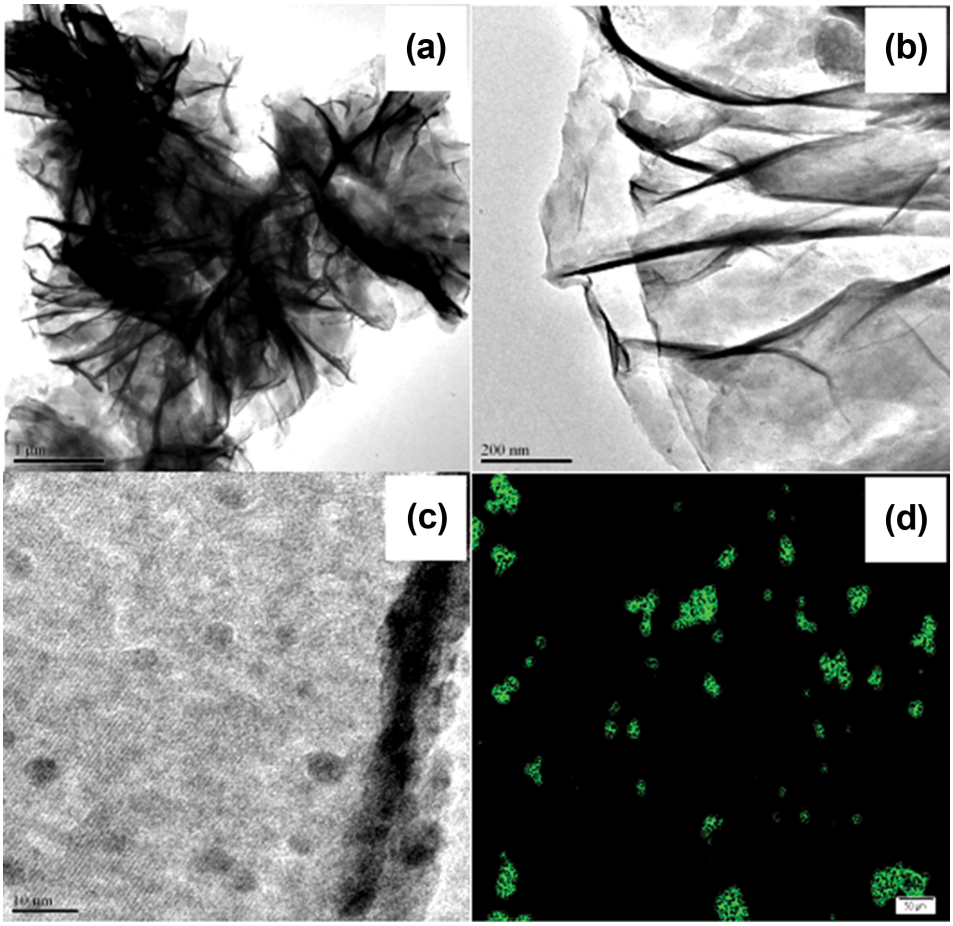


Fig. 6. TEM images of PVAase hybrid nanoflowers at different magnifications (a), (b), (c). CLSM of PVAase hybrid nanoflowers (d).

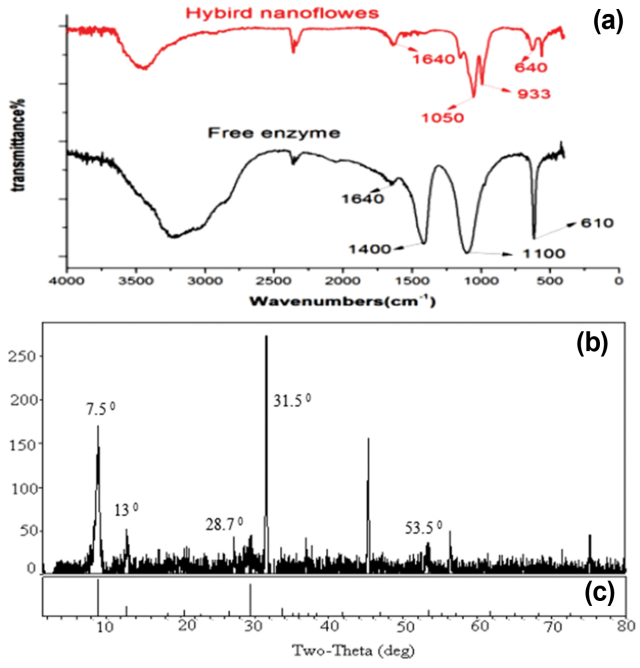


Fig. 7. FTIR spectra (a) of PVAase hybrid nanoflowers and XRD patterns of PVAase hybrid nanoflowers (b) and standard $Cu_3(PO_4)_2 \cdot 3H_2O$ (JPSCD 00-022-0548) (c).

With increase of PVAase concentration, activity of the PVAase hybrid nanoflowers increased. The maximum activity of the PVAase hybrid nanoflowers was obtained when PVAase concentration was 0.25 mg/mL. Furthermore, the PVAase hybrid nanoflowers exhibited high protein loading capacity (21 wt%). Note that the PVAase hybrid nanoflowers exhibited uniform nanoflowers at 0.25 mg/mL. These results indicated that the activity of hybrid nanoflowers depended not only on the shape of hybrid nanoflowers, but also on the quantity of enzyme used. Similarly, it could be found that PVAase hybrid nanoflowers exhibited their high activities when Cu^{2+} concentration and incubation time were at 0.36 mM and 72 h, respectively (Fig. 8(b), and 8(c)). The maximal PVAase activity recovery in the PVAase hybrid nanoflowers was approximately 85% at 0.25 mg/mL PVAase, 0.36 mM copper ions, and 72 h incubation time (data not shown). Generally, pH and temperature are the critical factors that may affect the enzyme performance [38], so we investigated the effects of pH and temperature on the hybrid nanoflowers. The maximum activity of both free PVAase and the PVAase hybrid nanoflowers was at 30 °C. However, the hybrid nanoflowers displayed higher activity than free PVAase in the range of 40-70 °C (Fig. 9(a)). Similarly, the optimum pH of both free PVAase and hybrid nanoflowers was 7.0; however, the PVAase hybrid nanoflowers maintained a relatively high activity in a broad pH range (Fig. 9(b)).

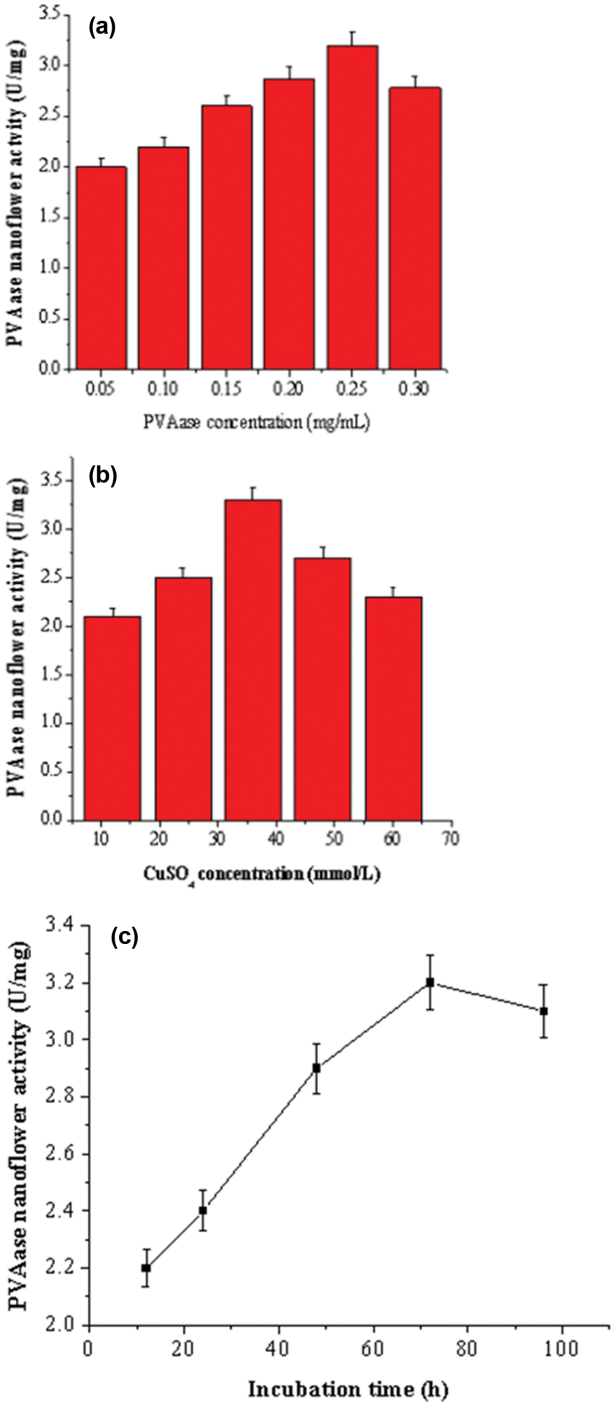


Fig. 8. Effects of PVAase concentration (a), $CuSO_4$ concentration (b), and incubation time (c) on activity of PVAase hybrid nanoflower.

3. Stability and Durability

In terms of stability, the thermostability and storage stability of PVAase hybrid nanoflowers were tested. The activity of free PVAase was significantly decreased after 1 h treatment at 50 °C (Fig. 10(a)). Complete inactivation could be observed when the incubation time reached 5 h. However, the PVAase hybrid nanoflower still retained 85% of its original activity. The results showed that the PVAase

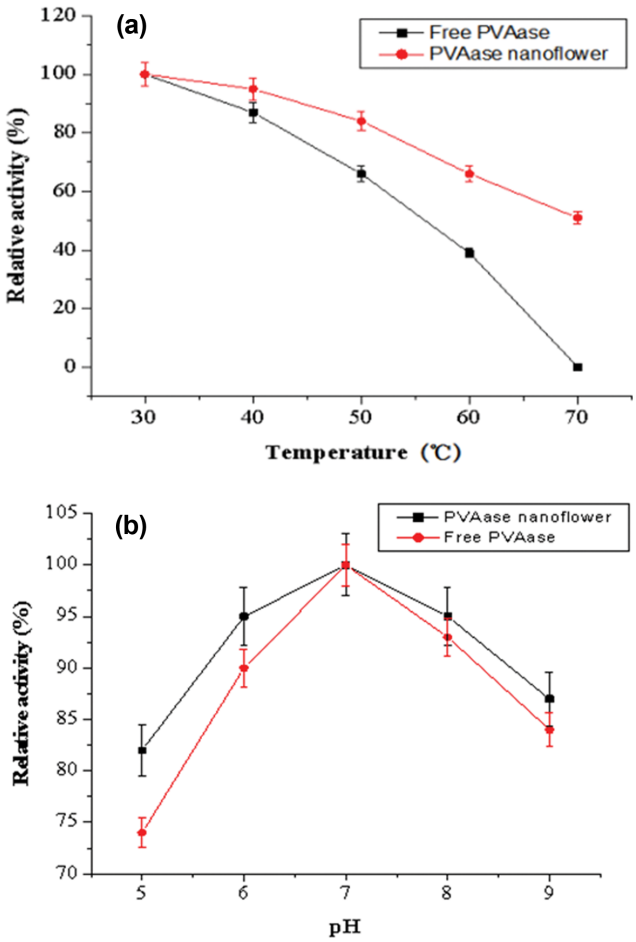


Fig. 9. Effects of temperature (a) and pH (b) on activity of PVAase hybrid nanoflowers.

hybrid nanoflower had higher thermal stability than free PVAase. This might be because the nanoflower petals protected encapsulated enzymes and maintained their active conformation at high temperatures. As shown in Fig. 10(b), free PVAase lost 90% of its original activity over six days. However, the PVAase hybrid nanoflower only lost 10% of its original activity under the same conditions, confirming the hybrid nanoflowers had superior tolerance to room temperature storage. In addition, reusability of the hybrid nanoflower was studied since the reuse efficiency is one of the key factors for immobilized enzymes application. It was found that the PVAase hybrid nanoflower only lost 10% of its original activity after 8 cycles (Fig. 11(a)). The slight decrease of PVAase activity might be attributed to the little leakage of PVAase caused by the separating and washing processes [26,39]. Furthermore, deformation in the morphology of PVAase hybrid nanoflower was not observed under SEM after eight cycles (data no shown), suggesting that the PVAase hybrid nanoflowers had excellent reusability and mechanical stability, which may facilitate the PVA degradation during a continuous operation. To test this hypothesis, PVA degradation efficiency of PVAase samples was tested. Total PVA degradation efficiency of the hybrid nanoflower reached 86.2%, whereas crude PVAase was only 46.5% (Fig. 11(b)), indicating that the hybrid nanoflowers had ability to degrade PVA continuously.

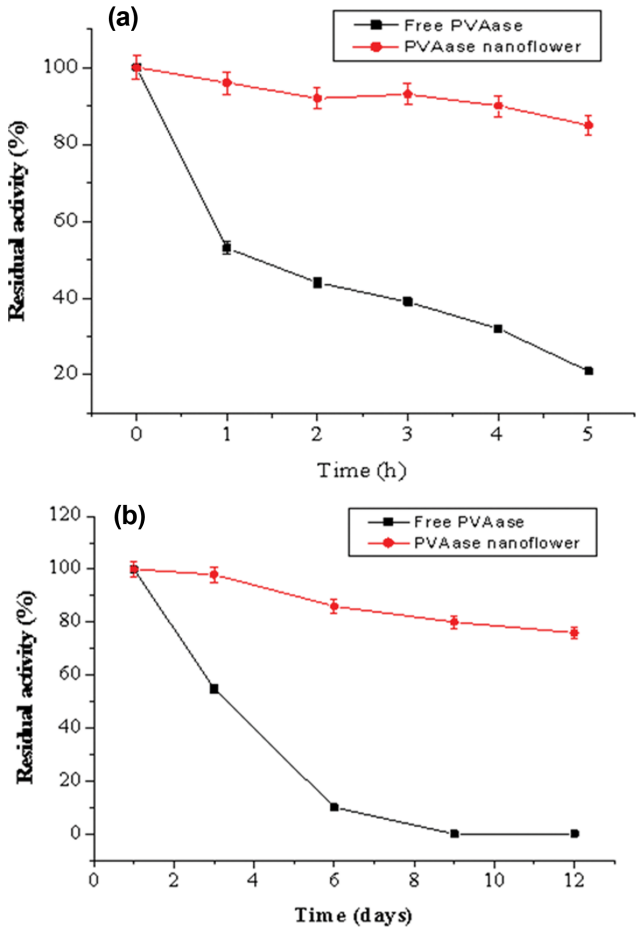


Fig. 10. Stability of PVAase hybrid nanoflowers. (a) Thermostability, (b) storage stability.

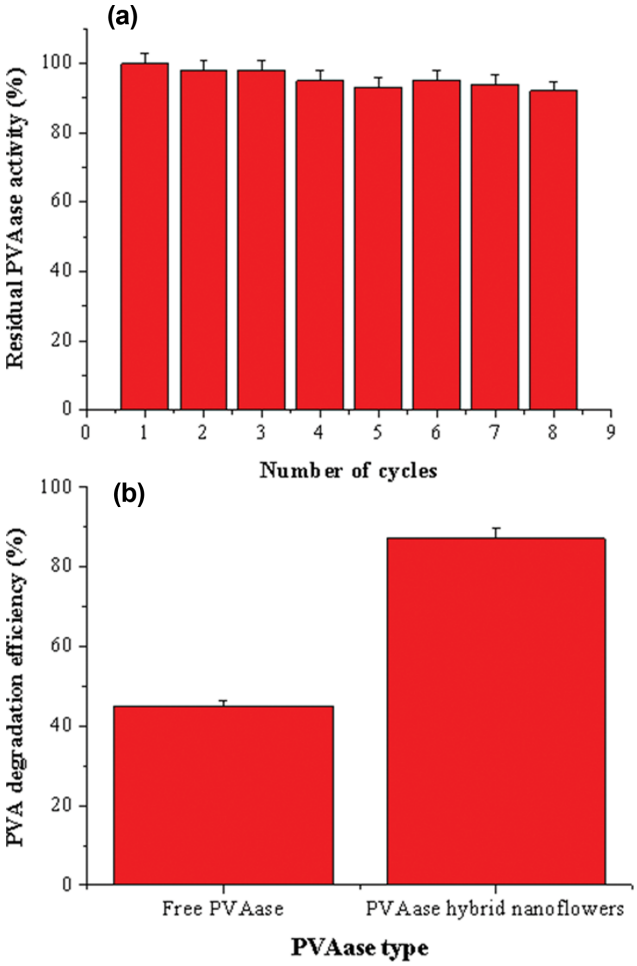


Fig. 11. Reusability of PVAase hybrid nanoflowers (a) and PVA degradation efficiency of PVAase hybrid nanoflowers (b).

CONCLUSIONS

PVAase-$Cu_3(PO_4)_2$ hybrid nanoflower was successfully synthesized using crude PVAase from *Bacillus niacini*, and used for PVA degradation. Analysis of SEM, TEM, XRD, and FTIR showed that the PVAase-$Cu_3(PO_4)_2$ hybrid composites had good flower-like morphology. The morphology and activity of hybrid nanoflower could be regulated by changing PVAase concentration, Cu^{2+} concentration, and incubation time. The resultant PVAase hybrid nanoflower exhibited high thermostability and storage stability compared with free PVAase. Furthermore, the hybrid nanoflower had excellent reusability and PVA degradability, indicating its potential application in PVA degradation.

ACKNOWLEDGEMENTS

This work is partially supported by the Open Project Program of State Key Laboratory of Food Nutrition and Safety, Tianjin University of Science & Technology (project no. SKLFNS-KF201904). Dr. J. D. Cui also thanks the support from the Key Projects of Tianjin Natural Science Foundation, China (project no. 19JCZDJC38100), and the Foundation (No. 19272809D) of Key R & D projects of science and Technology Department of Hebei Province.

REFERENCES

1. S. Tsujiyama and A. Okada, *Biotechnol. Lett.*, **35**, 1907 (2013).
2. N. B. Halima, *RSC Adv.*, **6**, 39823 (2016).
3. Y. L. Liu, Y. L. Deng, P. Chen, M. J. Duan, X. S. Lin and Y. Zhang, *J. Basic. Microbiol.*, **59**, 368 (2019).
4. R. K. Balasubramanian, *Colloids Surf. A*, **455**, 174 (2014).
5. M. N. Kim and M. G. Yoon, *Polym. Degrad. Stab.*, **95**, 89 (2010).
6. A. Stoica-Guzun, L. Jecu, A. Gheorghe, I. Raut, M. Stroescu, M. Ghiurea, M. Danila, I. Jipa and V. Fruth, *J. Polym. Environ.*, **19**, 69 (2011).
7. E. Chiellini, A. Corti, S. D'Antone and R. Solaro, *Prog. Polym. Sci.*, **28**, 963 (2003).
8. N. B. Halima, *RSC Adv.*, **6**, 39823 (2016).
9. T. Suzuki, Y. Ichihara, M. Yamada and K. Tonomura, *Agric. Biol. Chem.*, **37**, 747 (1973).
10. T. Tsujiyama and T. Maoka Nitta, *J. Biosci. Bioeng.*, **112**, 58 (2011).
11. H. J. Bian, M. F. Cao, H. Wen, Z. L. Tan, S. R. Jia and J. D. Cui, *Int. J. Biol. Macromol.*, **124**, 10 (2019).
12. M. Ullah, C. H. Weng, H. Li, S. W. Sun, H. Zhang, A. H. Song and H. Zhu, *Environ. Technol.*, **39**, 2056 (2018).
13. M. Shimao, T. Tamogami and S. Kishida, *Microbiology*, **146**, 649

(2000).
14. Y. H. Wei, J. Fu, J. Y. Wu, X. Y. Jia, Y. H. Zhou, C. D. Li, M. X. Dong, S. S. Wang, J. Zhang and F. Chen, *Appl. Eviron. Microbial.*, **84**, e01898-17 (2018).
15. Y. Yang, D. X. Zhang, S. Liu, D. X. Jia, G. C. Du and J. Chen, *J. Ind. Microbiol. Biotechnol.*, **39**, 99 (2012).
16. D. X. Jia, J. H. Li, L. Liu, D. X. Zhang, Y. Yang, G. C. Du and J. Chen, *Appl. Microbiol. Biotechnol.*, **97**, 1113 (2013).
17. B. Tang, X. Y. Liao, D. X. Zhang, M. Li, R. Li, K. L. Yan, G. C. Du and J. Chen, *Polym. Degrad. Stab.*, **95**, 557 (2010).
18. L. Min, D. X. Zhang, G. C. Du and J. Chen, *J. Microbiol. Biotechnol.*, **22**, 220 (2012).
19. S. Z. Ren, C. H. Li, X. B. Jiao, S. R. Jia, Y. J. Jiang, M. Bilal and J. D. Cui, *Chem. Eng. J.*, **373**, 1254 (2019).
20. Z. Lin, Y. Xiao, L. Wang, Y. Q. Yin, J. N. Zheng, H. H. Yang and G. N. Chen, *RSC Adv.*, **4**, 13888 (2014).
21. J. Ge, J. D. Lei and R. N. Zare, *Nat. Nanotechnol.*, **7**, 428 (2012).
22. Z. Lin, Y. Xiao, Y. Q. Yin, W. L. Hu, W. Liu and H. H. Yang, *ACS Appl. Mater. Interfaces*, **6**, 10775 (2014).
23. B. Somturk, M. Hancer, I. Ocsoy and N. Ozdemir, *DALTON T.*, **44**, 13845 (2015).
24. B. L. Zhang, P. T. Li, H. P. Zhang, L. L. Fan, H. Wang, X. J. Li, L. Tian, N. Ali, Z. Ali and Q. Y. Zhang, *RSC Adv.*, **6**, 46702 (2016).
25. J. D. Cui, Y. M. Zhao, R. L. Liu, C. Zhong and S. R. Jia, *Sci. Rep.*, **6**, 27928 (2016).
26. Z. F. Wu, H. Li, X. J. Zhu, S. Li, Z. Wang, L. Wang, Z. Q. Li and G. Ch, *Catalyst*, **7**, 188 (2017).
27. K. Qian, H. Wang, J. M. Liu, S. T. Gao, W. T. Liu, X. Wan, Y. Y. Zhang, Q. S. Liu and X. Y. Yin, *New J. Chem.*, **42**, 429 (2018).
28. Y. Yu, X. Fei, J. Tian, L. Q. Xu, X. Y. Wang and Y. Wang, *Colloids Surf. B.*, **130**, 299 (2015).
29. M. Zhao, J. H. Rong, J. Han, Y. Zhou, C. M. Li, L. Wang, Y. L. Mao and Y. Wang, *ACS Appl. Mater. Interfaces*, **11**, 31878 (2019).
30. M. M. Bradford, *Anal. Biochem.*, **72**, 248 (1976).
31. J. H. Finley, *Anal. Chem.*, **33**, 1925 (1961).
32. S. Escobar, S. Velasco-Lozano, C. H. Lu, Y. F. Lin, M. Mesa, C. Bernal and F. Lopez-Gallego, *J. Mater. Chem. B.*, **5**, 4478 (2017).
33. S. W. Lee, S. A. Cheon, M. I. Kim and T. J. Park, *J. Nanobiotechnol.*, **13**, 54 (2015).
34. U. Q. Yin, Y. Xiao, G. Lin, Q. Xiao, Z. Lin and Z. W. Cai, *J. Mater. Chem. B.*, **3**, 2295 (2015).
35. C. Altinkaynak, I. Yilmaz, Z. Koksal, H. Ozdemir, I. Ocsoy and N. Ozdemir, *Int. J. Biol. Macromol.*, **84**, 402 (2016).
36. B. L. Zhang, P. T. Li, H. P. Zhang, H. Wang, X. J. Li, L. Tian, N. Ali, Z. Ali and Q. Y. Zhang, *Chem. Eng. J.*, **291**, 287 (2016).
37. A. Baldemir, N. B. Kose, N. Ildiz, S. Ilgun, S. Yusufbeyoglu, V. Yilmaz and I. Ocsoy, *RSC Adv.*, **7**, 44303 (2017).
38. R. C. Rodrigues, C. Ortiz, Á. Berenguer-Murcia, R. Torres and R. Fernández-Lafuente, *Chem. Soc. Rev.*, **42**, 6290 (2013).
39. S. Yabuki, *Catalyst*, **7**, 36 (2017).